Relating Granger causality to long-term causal effects

Dmitry A. Smirnov[1,2,*] and Igor I. Mokhov[3,2,†]

[1]*Saratov Branch of V.A. Kotel'nikov Institute of RadioEngineering and Electronics of the Russian Academy of Sciences, 38 Zelyonaya St., Saratov 410019, Russia*

[2]*Institute of Applied Physics of the Russian Academy of Sciences, 46 Ulyanova St., Nizhny Novgorod 603950, Russia*

[3]*A.M. Obukhov Institute of Atmospheric Physics of the Russian Academy of Sciences, 3 Pyzhevsky, Moscow 119017, Russia*

(Received 2 April 2015; revised manuscript received 7 September 2015; published 16 October 2015)

In estimation of causal couplings between observed processes, it is important to characterize coupling roles at various time scales. The widely used Granger causality reflects short-term effects: it shows how strongly perturbations of a current state of one process affect near future states of another process, and it quantifies that via prediction improvement (PI) in autoregressive models. However, it is often more important to evaluate the effects of coupling on long-term statistics, e.g., to find out how strongly the presence of coupling changes the variance of a driven process as compared to an uncoupled case. No general relationships between Granger causality and such long-term effects are known. Here, we pose the problem of relating these two types of coupling characteristics, and we solve it for a class of stochastic systems. Namely, for overdamped linear oscillators, we rigorously derive that the above long-term effect is proportional to the short-term effects, with the proportionality coefficient depending on the prediction interval and relaxation times. We reveal that this coefficient is typically considerably greater than unity so that small normalized PI values may well correspond to quite large long-term effects of coupling. The applicability of the derived relationship to wider classes of systems, its limitations, and its value for further research are discussed. To give a real-world example, we analyze couplings between large-scale climatic processes related to sea surface temperature variations in equatorial Pacific and North Atlantic regions.

DOI: 10.1103/PhysRevE.92.042138 PACS number(s): 02.50.Tt, 05.45.Tp, 05.45.Xt, 02.50.Ey

I. INTRODUCTION

Revealing directional (causal) couplings between elements of complex systems from observed time series is an important step toward a better understanding of their collective behavior and to a more accurate prediction of their evolution under changing conditions. Therefore, the problem of causal coupling estimation is widely encountered in physics [1–6], engineering [7–9], ecology [10], climate science [11–17], neuroscience [18–22], and other fields. Moreover, it continues to attract attention; see, e.g., a series of recent papers of different groups in two subsequent issues [23–28]. An especially important aspect deserving more detailed studies is a characterization of the role of coupling at different time scales [17,29–31], including a distinction between shorter- and longer-term causal effects [28,32].

The basic idea underlying most of the above-mentioned techniques is the concept of Granger causality [33,34]: one compares how uncertainty about the future of one process is changed if the past data from another process are taken into account. It is typically implemented via fitting autoregressive (AR) models to a time series and calculating one-step-ahead or several-steps-ahead prediction improvement (PI) in terms of prediction error variance [33]. A measure as popular as transfer entropy [35] and its various modifications [15,21,22,36,37] can be viewed as elaborate implementations of the same concept. Although this approach can lead to spurious detection of couplings under certain conditions [38–40] where additional tests are required [39], in a broad range of situations it appears to be quite an efficient tool for coupling detection from relatively short and noisy signals. An overview of its recent applications to climate data is given in Ref. [41].

A desired step beyond coupling detection is the quantification of coupling "strength" or "importance," which is much more difficult [28]. In physical problems, it is often necessary to understand the overall role of coupling in dynamics, e.g., one should determine how strongly one process contributes to variance or another long-term statistic of the second process due to their coupling [28,42]. It would be highly desirable to interpret concrete numerical values of PIs in such terms, but it remains unknown how to do that. In practice, normalized PIs estimated from time series are often statistically significant, but they take on small values of about 1–2% [12,13]. Does this mean that the effects of couplings on long-term characteristics are of the same order and may be considered as a secondary circumstance? Or, in contrast, can a small PI correspond to the rather considerable long-term role of coupling? If we were able to answer these questions and relate PI to such a long-term contribution of coupling, Granger causality analysis would become much more useful for a quantitative characterization of couplings. This is especially so because reliable direct estimation of the long-term role of coupling is problematic, contrary to the well-established techniques for PI estimation.

To put the posed questions in a wider context and justify the terms used throughout the paper, we note that Granger causality is closely related to a finite-time (one step ahead or several steps ahead depending on the prediction interval used) causal effect, which shows how strongly an initial state of one process influences near future states of another process [28,43,44]. If both processes under study are characterized by individual relaxation times beyond which any dependence of their states on the initial conditions disappears, informative PI values are obtained for prediction intervals that do not strongly exceed those characteristic time scales. Therefore, we call such

*smirnovda@yandex.ru
†mokhov@ifaran.ru

characteristics "short-term effects." In contrast, if one studies how stationary statistics of a process vary in response to a change in coupling (i.e., to a change in a constant parameter rather than in an initial state), the resulting characteristics describe the properties that are clearly manifest in a time series whose duration is much longer than all the characteristic time scales of the processes. Therefore, herein such characteristics are called "long-term effects." Similar types of characteristics have been recognized and mentioned in previous works. For example, within the context of numerical atmospheric circulation models [45], predictions of the near future states depending on the initial state have been called "predictions of the first kind," while predictions of how stationary statistics of a process vary if a certain parameter is changed have been called "predictions of the second kind." The problem of relating the short-term and long-term effects of directional couplings is posed here.

Within the framework of dynamical causal effects [28], Granger causality falls into the "state space intervention–orbital effect" family of coupling characteristics, while the change in stationary variance of a process in response to zeroing of the respective coupling coefficient belongs to the "parametric intervention–stationary effect" family. It has been argued that such short-term and long-term effects are irreducible to each other in general [28]. However, it can be expected that they are closely related within certain classes of systems, the form of their relationship depending on the properties of such a class. Therefore, it seems fruitful to start a study of those relationships from a reasonably simple and still informative set of systems. Following this idea, we perform here a complete rigorous analysis of the relationship between the above long-term effect and short-term ones for a class of linear stochastic systems, namely for overdamped oscillators. We reveal that this is a proportionality relationship for moderate coupling strengths, and we find an exact dependence of the proportionality coefficient on the relaxation times of the oscillators. A possible wider applicability of the derived simple relationship and its limitations are further discussed. To give a concrete real-world illustration of the theoretical results, we estimate short-term and long-term effects of couplings between large-scale climate processes of global importance related to sea surface temperature variations in the Pacific and Atlantic Oceans.

The paper is organized as follows. Section II reviews the definition of Granger causality. Section III describes a short-term "intervention–effect" characteristic that helps to link PIs to long-term causal effects. The latter are introduced in Sec. IV. Section V contains a derivation of the relationships between the short-term and long-term effects and a discussion of its results. A climate data analysis is presented in Sec. VI. Conclusions are given in Sec. VII.

II. GRANGER CAUSALITY

The basic problem considered below is the following. There are two systems X and Y that may be coupled, either in a uni- or a bidirectional way. One observes time series of two scalar variables u and v representing the dynamics of X and Y, respectively. The task is to reveal and quantify directional couplings between X and Y from the observed data.

To introduce mathematical definitions, we assume that an observed time series is a realization of a stationary bivariate random process $[U(t),V(t)]$: $u_n = U(t_n)$ and $v_n = V(t_n)$, where $t_n = n\Delta t$, Δt is sampling interval, and n is an integer. Let us denote the values of u and v preceding time t_n as $\mathbf{u}_n^- = (u_{n-1},u_{n-2},\dots)$ and $\mathbf{v}_n^- = (v_{n-1},v_{n-2},\dots)$. To characterize the influence $X \to Y$, consider conditional distributions $\rho(v_n|\mathbf{v}_n^-)$ and $\rho(v_n|\mathbf{u}_n^-,\mathbf{v}_n^-)$. If $\rho(v_n|\mathbf{v}_n^-)$ differs from $\rho(v_n|\mathbf{u}_n^-,\mathbf{v}_n^-)$ at any $\mathbf{u}_n^-$ and $\mathbf{v}_n^-$, then the system X is said to "Granger cause" the system Y. Multiple-step-ahead conditional distributions can also be studied [34], but the above one-step-ahead characteristics often suffice for correct coupling detection.

As a general measure of the distance between the distributions $\rho(v_n|\mathbf{v}_n^-)$ and $\rho(v_n|\mathbf{u}_n^-,\mathbf{v}_n^-)$, one can use Kullback-Leibler divergence and arrive at transfer entropy [35]. For Gaussian processes, this is equivalent to comparing the respective conditional variances. Due to the simplicity of the latter characteristic, it is often applied to non-Gaussian processes as well [46] and is used as the Granger causality measure below. Namely, let v_n^{ind} be the "self-predictor" of v_n given by $v_n^{\mathrm{ind}} = E[v_n|\mathbf{v}_n^-]$, where $E[\cdot|\cdot]$ stands for a conditional expectation. The mean-squared prediction error $\sigma^2_{v,\mathrm{ind}} = E[(v_n - v_n^{\mathrm{ind}})^2]$ represents the conditional variance and is minimal over all self-predictors. The joint predictor $v_n^{\mathrm{joint}} = E[v_n|\mathbf{u}_n^-,\mathbf{v}_n^-]$ gives the error $\sigma^2_{v,\mathrm{joint}}$, which is minimal over all joint predictors. Then, the normalized PI value $G_{X\to Y} = (\sigma^2_{v,\mathrm{ind}} - \sigma^2_{v,\mathrm{joint}})/\sigma^2_{v,\mathrm{ind}}$ characterizes Granger causality in the direction $X \to Y$ and ranges from 0 to 1. In application to Gaussian processes, the idea is realized [33] through the bivariate linear AR description,

$$\begin{aligned} u_n &= \sum_{k=1}^{d_X} a_{u,k}u_{n-k} + \sum_{k=1}^{d_{XY}} b_{u,k}v_{n-k} + \xi_n, \\ v_n &= \sum_{k=1}^{d_Y} a_{v,k}v_{n-k} + \sum_{k=1}^{d_{YX}} b_{v,k}u_{n-k} + \psi_n, \end{aligned} \tag{1}$$

where (ξ_n,ψ_n) is a bivariate zero-mean Gaussian white noise with variances σ_ξ^2 and σ_ψ^2 and covariance $E[\xi_n\psi_n] = \gamma$. Any bivariate stationary Gaussian process is uniquely represented in the form (1) where, in general, infinite orders d_X, d_{XY}, d_Y, and d_{YX} are required to provide whiteness of the noise. This whiteness assures that $\sigma_\xi^2 = \sigma^2_{u,\mathrm{joint}}$ and $\sigma_\psi^2 = \sigma^2_{v,\mathrm{joint}}$ [47]. Similarly, the unique univariate AR description of the process v_n is given by the second line in Eqs. (1) with $d_{YX} = 0$ and a different white noise ψ'_n with variance $\sigma^2_{\psi'} = \sigma^2_{v,\mathrm{ind}}$. Now, one determines $G_{X\to Y} = (\sigma^2_{\psi'} - \sigma_\psi^2)/\sigma^2_{\psi'}$. Everything is similar for $G_{Y\to X}$.

In the theoretical analysis of Sec. V, we mainly use PIs divided by the smallest variance $G'_{X\to Y} = (\sigma^2_{v,\mathrm{ind}} - \sigma^2_{v,\mathrm{joint}})/\sigma^2_{v,\mathrm{joint}}$ for convenience. It holds that $G'_{X\to Y} = G_{X\to Y}/(1 - G_{X\to Y})$ so that $G'_{X\to Y} \approx G_{X\to Y}$ when both quantities are considerably smaller than unity.

To estimate $G_{X\to Y}$ and $G_{Y\to X}$ from a finite time series $\{u_n,v_n\}_{n=1}^N$, one can use well-established techniques based on fitting univariate and bivariate AR models to that time series (Sec. VI). For nonlinear systems, one can proceed in a similar way and use nonlinear AR models to define PIs [46]. The nonlinear case is only briefly commented on in Sec. V D.

III. SHORT-TERM CAUSAL EFFECTS

Granger causality characteristics are of informational character and do not quantify causal effects directly, but they are closely related to short-term causal effects [2,28], which is justified in this section in some detail. It is relevant to recall the families of coupling characteristics introduced in Ref. [28] for state space systems to quantify causal influences in terms of "intervention-dynamical effect." Let us consider systems X and Y specified by stochastic differential equations,

$$\begin{aligned} \dot{\mathbf{x}} &= \mathbf{f}_X(\mathbf{x},\mathbf{y}) + \xi_X(t), \\ \dot{\mathbf{y}} &= \mathbf{f}_Y(\mathbf{y},\mathbf{x}) + \xi_Y(t), \end{aligned} \tag{2}$$

where $\mathbf{x}$ and $\mathbf{y}$ are state vectors of the systems, functions $\mathbf{f}_X$ and $\mathbf{f}_Y$ represent both internal dynamics and coupling, and ξ_X and ξ_Y are mutually independent Gaussian white noises. We assume that the scalar observables u and v are single-valued functions of the respective states $u = u(\mathbf{x})$ and $v = v(\mathbf{y})$, and we denote by $\rho_t(v|\mathbf{x}_0,\mathbf{y}_0)$ the conditional probability density of the variable v at time t, given the initial state $(\mathbf{x}_0,\mathbf{y}_0)$ at time $t_0 = 0$.

In the spirit of Ref. [28], a finite-time causal effect $X \to Y$ with respect to the variable v can be defined through a change in $\rho_t(v|\cdot)$, which occurs if an initial state of X is changed from $\mathbf{x}_0$ to $\mathbf{x}_0^*$, given $\mathbf{y}_0$. The normalized effect reads

$$F_{X\to Y}(t,\mathbf{x}_0,\mathbf{x}_0^*,\mathbf{y}_0) = \frac{|E[v(t)|\mathbf{x}_0,\mathbf{y}_0] - E[v(t)|\mathbf{x}_0^*,\mathbf{y}_0]|}{\sqrt{\mathrm{var}[v(t)|\mathbf{x}_0,\mathbf{y}_0] + \mathrm{var}[v(t)|\mathbf{x}_0^*,\mathbf{y}_0]}}, \tag{3}$$

where the denominator is used to measure the difference in conditional expectations in terms of the respective conditional variances to quantify a separation of the conditional distributions. Such a change in the state of X has been called "intervention" [43] or "state space intervention" [28]. Such an effect has been called "orbital" [28] since it shows how phase orbits $\mathbf{y}(t)$ emanating from $\mathbf{y}_0$ (and projected to the variable v) shift in response to the intervention. The resulting characteristic belongs to the family "state space intervention–orbital effect" [28]. Averaging over $\rho(\mathbf{y}_0)\rho(\mathbf{x}_0|\mathbf{y}_0)\rho(\mathbf{x}_0^*|\mathbf{y}_0)$, where $\rho(\mathbf{y})$ is a stationary distribution of $\mathbf{y}$ and $\rho(\mathbf{x}|\mathbf{y})$ a distribution of $\mathbf{x}$ conditioned by simultaneous $\mathbf{y}$, one gets

$$F_{X\to Y}(t) = \sqrt{\left\langle F_{X\to Y}^2(t,\mathbf{y}_0,\mathbf{x}_0,\mathbf{x}_0^*)\right\rangle_{\mathbf{y}_0,\mathbf{x}_0,\mathbf{x}_0^*}}, \tag{4}$$

where the angular brackets denote the averaging. This kind of averaging means that the vectors $\mathbf{x}_0$ and $\mathbf{x}_0^*$ are drawn from the conditional distribution independently of each other. In a free run, the system returns many times to close neighborhoods of the states $(\mathbf{x}_0,\mathbf{y}_0)$ and $(\mathbf{x}_0^*,\mathbf{y}_0)$ and, thereby, naturally "compares" orbit beams emanating from these two states. For the stochastic system (2), $F_{X\to Y}(t)$ is small for small t, reaches its maximal values for some intermediate t close to characteristic time scales of X and Y, and quickly decreases at greater times [28]. Let us denote that maximal value $F_{X\to Y,\max} = \max_{t>0} F_{X\to Y}(t)$ and the respective time $t_{X\to Y,\max} = \arg\max_{t>0} F_{X\to Y}(t)$. Since all these F measures quantify finite-time effects at moderate times t, we call them "short-term causal effects."

To provide a link with Granger causality, let us denote the conditional variance of $v(\Delta t)$ at a given initial state of Y as $\mathrm{var}[v(\Delta t)|\mathbf{y}_0]$. It equals a minimal mean-squared prediction error over all predictors based only on the initial state of Y. If $\mathrm{var}[v(\Delta t)|\mathbf{x}_0,\mathbf{y}_0]$ is independent of the initial state $(\mathbf{x}_0,\mathbf{y}_0)$, as is the case for linear stochastic systems, then one gets $F_{X\to Y}(\Delta t) = \{\mathrm{var}[v(\Delta t)|\mathbf{y}_0] - \mathrm{var}[v(\Delta t)|\mathbf{x}_0,\mathbf{y}_0]\}/\mathrm{var}[v(\Delta t)|\mathbf{x}_0,\mathbf{y}_0]$, which is a direct analog of $G'_{X\to Y}$, where the predictors $\mathbf{u}_n^-$ and $\mathbf{v}_n^-$ are analogs of the states $\mathbf{x}_0$ and $\mathbf{y}_0$. In the case of sufficiently weak couplings and not too sparse sampling, the states $\mathbf{x}(t_{n-1})$ and $\mathbf{y}(t_{n-1})$ are well represented by the observed vectors $\mathbf{u}_n^-$ and $\mathbf{v}_n^-$, respectively [39,40]. Then, one gets $F_{X\to Y}^2(\Delta t) \approx G'_{X\to Y}$, i.e., PI can be used as a proxy for the finite-time causal effect over the prediction interval Δt. In particular, it is valid for the examples studied in Sec. V.

IV. LONG-TERM CAUSAL EFFECTS

To characterize an "overall contribution" of the coupling $X \to Y$ to the observed dynamics of Y, one can assess changes in statistical properties of the process $v(t)$ that would occur if the coupling $X \to Y$ were "switched off." Similarly to regression analysis [45,48,49], we focus on assessing the change in stationary variance. For a concrete definition, an explicit coupling parameter dependence must be considered [28], e.g., as follows:

$$\begin{aligned} \dot{\mathbf{x}} &= \mathbf{F}_X(\mathbf{x}) + c_{XY}\mathbf{G}_X(\mathbf{x},\mathbf{y}) + \xi_X(t), \\ \dot{\mathbf{y}} &= \mathbf{F}_Y(\mathbf{y}) + c_{YX}\mathbf{G}_Y(\mathbf{y},\mathbf{x}) + \xi_Y(t), \end{aligned} \tag{5}$$

where $\mathbf{F}_X$ and $\mathbf{F}_Y$ describe the internal dynamics of the systems X and Y, $\mathbf{G}_X$ and $\mathbf{G}_Y$ are coupling functions, and c_{XY} and c_{YX} are coupling coefficients. If $c_{YX} = 0$ ($c_{XY} = 0$), the system Y (X) evolves independently of X (Y). Let us denote the stationary variance of v at given values of coupling coefficients c_{XY}^* and c_{YX}^* as $\sigma_v^2(c_{XY}^*,c_{YX}^*)$. If the influence $X \to Y$ is suppressed, i.e., if one sets $c_{YX} = 0$ instead of $c_{YX} = c_{YX}^*$, then the variance of v equals $\sigma_v^2(c_{XY}^*,0)$. The latter is a "free" variance of v, which can be denoted $\sigma_{v,0}^2$. Then, the contribution of the coupling $X \to Y$ to the variance $\sigma_v^2(c_{XY}^*,c_{YX}^*)$ is defined [28,42] as

$$S_{X\to Y} = \frac{\sigma_v^2(c_{XY}^*,c_{YX}^*) - \sigma_{v,0}^2}{\sigma_{v,0}^2}. \tag{6}$$

This characteristic belongs to the family "parametric intervention–stationary effect" [28]. Since it quantifies a change in a stationary statistic that manifests itself only in the long-term behavior, i.e., over a time interval including many characteristic time scales of the system, we call it the "long-term causal effect."

By using the denominator $\sigma_v^2(c_{XY}^*,c_{YX}^*)$ instead of $\sigma_{v,0}^2$ in Eq. (6), one gets the quantity $\tilde{S}_{X\to Y} = S_{X\to Y}/(1 + S_{X\to Y})$ to assess which part of the variance $\sigma_v^2(c_{XY}^*,c_{YX}^*)$ is "determined" by the coupling $X \to Y$. This is meaningful if the numerator is positive. However, the numerator can be negative for bidirectionally coupled systems (Sec. V C), making the interpretation in terms of the variance decomposition irrelevant. Still, a "unidirectional" long-term effect can be defined via a comparison of the variance of v for zero and nonzero coupling

$X \to Y$ under the additional condition $c^*_{XY} = 0$:

$$S^{\text{uni}}_{X\to Y} = \frac{\sigma_v^2(0,c^*_{YX}) - \sigma^2_{v,0}}{\sigma^2_{v,0}}. \tag{7}$$

It shows how strongly the variance of v would change as compared to the uncoupled case if only the unidirectional coupling $X \to Y$ were "switched on" rather than both couplings $X \to Y$ and $Y \to X$ together, as in Eq. (6). In the examples of Sec. V, $S^{\text{uni}}_{X\to Y}$ is positive and can be interpreted as a "unidirectional effect" of coupling on the variance of v. Similar characterizations are familiar in physics, e.g., a scheme with excluded feedbacks is used in analysis of numerical atmospheric and oceanic circulation models to estimate the mutual influence of sea surface temperature variations and monsoon circulation [45].

A direct approach to the estimation of $S_{X\to Y}$ from a time series $\{u_n, v_n\}$ can be based on the obtained bivariate AR model (1) used as a proxy of the processes under study. Namely, one can assume that "switching the coupling $X \to Y$ off" in the original system would correspond to zeroing all the coefficients $b_{v,k}$ in Eqs. (1) with all other parameters unchanged. Under this assumption, the variance of v in the model at zero and nonzero couplings and, thereby, $S^{\text{uni}}_{X\to Y}$ and $S_{X\to Y}$ can be calculated [42]. In other words, one extrapolates the AR model obtained for coupled systems to the zero-coupling case. This is not a unique idea, e.g., a similar extrapolation of empirical models in parameter space has been used to predict possible bifurcations in El – Niño dynamics [50]. However, extrapolation is often a problematic step, and its validity is not always assured. Therefore, it is desirable to have an alternative way to estimate the long-term effects, e.g., by finding their relationships with PIs.

We note that the above long-term effects differ from the widely used notion of "long-range correlations." The latter imply that a system exhibits characteristic time scales of different orders of magnitude, and its autocorrelations at large times decay slowly. It may lead to considerable $F_{X\to Y}(t)$ at relatively large times t. The latter are still finite-time and, in our terminology, relatively "short-term" as compared to S characteristics that quantify changes in stationary distributions manifest over time intervals significantly exceeding all characteristic time scales. However, consideration of systems with multiple time scales is beyond the scope of this paper, as discussed in Sec. V D.

V. RELATIONSHIPS BETWEEN SHORT-TERM AND LONG-TERM EFFECTS

To relate short-term causal effects $F_{X\to Y}(t)$ and $F_{X\to Y,\max}$ to long-term causal effects $S_{X\to Y}$ and $S^{\text{uni}}_{X\to Y}$, we consider one-dimensional linear stochastic systems X and Y called overdamped oscillators or relaxation systems:

$$\begin{aligned} \dot{x} &= -\alpha_X x + c_{XY} y + \xi_X(t), \\ \dot{y} &= -\alpha_Y y + c_{YX} x + \xi_Y(t), \end{aligned} \tag{8}$$

where x and y are state variables, $\alpha_X > 0$ and $\alpha_Y > 0$ are damping coefficients, c_{XY} and c_{YX} are coupling coefficients, and $\xi_X(t)$ and $\xi_Y(t)$ are mutually independent zero mean Gaussian white noises with covariance functions $\langle \xi_X(t_1)\xi_X(t_2)\rangle = \Gamma_{XX}\delta(t_1 - t_2)$ and $\langle \xi_Y(t_1)\xi_Y(t_2)\rangle = \Gamma_{YY}\delta(t_1 - t_2)$, where δ is a Dirac delta, $\Gamma_{XX} > 0$, and $\Gamma_{YY} > 0$. The observables are $u = x$ and $v = y$. Individual relaxation times are $\tau_X = 1/\alpha_X$ and $\tau_Y = 1/\alpha_Y$, mean relaxation speed is $\bar{\alpha} = (\alpha_X + \alpha_Y)/2$, and mean relaxation time is $\bar{\tau} = 1/\bar{\alpha}$.

An advantage of using the system (8) as the basis to solve the posed problem is that it makes possible an in-depth and complete rigorous analysis with vivid simple results. At the same time, its consequences are of more general value and are potentially useful for a broader range of systems, as discussed in Sec. V D. Below, we first give the necessary formulas and notations (Sec. V A) and then consider unidirectional coupling $X \to Y$ (Sec. V B) and a more complicated case of bidirectional coupling (Sec. V C).

A. General formulas and auxiliary notations

To determine the short-term effect $F_{X\to Y}(t)$, we find the conditional expectation and variance of $y = v$ in Eq. (3) by solving the linear equations (see, e.g., Ref. [28])

$$\begin{aligned} \dot{M}_X &= -\alpha_X M_X + c_{XY} M_Y, \\ \dot{M}_Y &= -\alpha_Y M_Y + c_{YX} M_Y, \end{aligned} \tag{9}$$

and

$$\begin{aligned} \dot{C}_{XX} &= -2\alpha_X C_{XX} + 2c_{XY} C_{XY} + \Gamma_{XX}, \\ \dot{C}_{XY} &= -(\alpha_X + \alpha_Y) C_{XY} + c_{YX} C_{XX} + c_{XY} C_{YY}, \\ \dot{C}_{YY} &= -2\alpha_Y C_{YY} + 2c_{YX} C_{XY} + \Gamma_{YY}, \end{aligned} \tag{10}$$

where $M_X(t) = E[x(t)|x_0, y_0]$, $M_Y(t) = E[y(t)|x_0, y_0]$, $C_{XX}(t) = \text{var}[x(t)|x_0, y_0]$, $C_{YY}(t) = \text{var}[y(t)|x_0, y_0]$, and $C_{XY}(t) = \text{cov}[x(t), y(t)|x_0, y_0]$ with initial conditions $M_X(0) = x_0$, $M_Y(0) = y_0$, and $C_{XX}(0) = C_{YY}(0) = C_{XY}(0) = 0$. General explicit solutions are possible but cumbersome, thus expressions for $F_{X\to Y}(t)$ and $F_{X\to Y}$ are presented below only for several typical cases. To evaluate Granger causality, we avoid its statistical estimation below and determine $G_{X\to Y}$ and $G_{Y\to X}$ precisely via finding time-lagged covariance matrices of the (X,Y) process from respective ordinary differential equations and computing the ratio of determinants of appropriate partial covariance matrices [40,51,52].

Stationary variances at given parameters and, hence, the long-term effects are found from Eq. (10) after setting the left-hand side equal to zero. The variances of x and y in the uncoupled case $c_{XY} = c_{YX} = 0$ equal $\sigma^2_{x,0} = \Gamma_{XX}/(2\alpha_X)$ and $\sigma^2_{y,0} = \Gamma_{YY}/(2\alpha_Y)$. The variance of $y = v$ in the coupled case is $\sigma^2_y = \sigma^2_{y,0} + \frac{\alpha_X c_{YX}}{(\alpha_X+\alpha_Y)(\alpha_X\alpha_Y - c_{XY}c_{YX})}(c_{YX}\sigma^2_{x,0} + c_{XY}\sigma^2_{y,0})$. The long-term effect then reads

$$S_{X\to Y} = \frac{\alpha_X c_{YX}\left(c_{YX}\sigma^2_{x,0} + c_{XY}\sigma^2_{y,0}\right)}{(\alpha_X + \alpha_Y)(\alpha_X\alpha_Y - c_{XY}c_{YX})\sigma^2_{y,0}}. \tag{11}$$

Hence, the unidirectional effect is $S^{\text{uni}}_{X\to Y} = \frac{c^2_{YX}\Gamma_{XX}}{(\alpha_X+\alpha_Y)\alpha_X\Gamma_{YY}}$. By introducing nondimensional parameters $m_{YX} = \alpha_Y/\alpha_X = \tau_X/\tau_Y$ (ratio of relaxation times) and $\beta_{YX} = \frac{c^2_{YX}\Gamma_{XX}}{\alpha^2_X\Gamma_{YY}}$ (normalized coupling parameter), one gets

$$S^{\text{uni}}_{X\to Y} = \frac{\beta_{YX}}{1 + m_{YX}}. \tag{12}$$

If $\beta_{YX} \ll 1$, then $S^{\rm uni}_{X\to Y} \ll 1$ and it can be shown that cross-correlation between x and y is also much less than unity. This case is close to what is typical in climate data analysis where one often faces small, but statistically significant cross-correlations (e.g., [12,13]). Below, we call the coupling $X \to Y$ with $\beta_{YX} \ll 1$ "weak," and we treat this case analytically. Then, we check the approximate validity of the obtained relationships between $S_{X\to Y}$ and $F^2_{X\to Y}(t)$ for moderate β_{YX}'s numerically.

B. Unidirectional coupling $X \to Y$

Solving Eqs. (9) and (10) at $c_{XY} = 0$ gives $F^2_{X\to Y}(t) = \frac{c^2_{YX}\sigma^2_{x,0}(1-\rho^2_{XY})(e^{-\alpha_Y t}-e^{-\alpha_X t})^2}{(\alpha_X-\alpha_Y)^2 C_{YY}(t)}$, where ρ_{XY} is zero-lag cross-correlation between $x(t)$ and $y(t)$. In general, $\rho^2_{XY} = \frac{m_{YX}\beta_{YX}}{(1+m_{YX})^2}$ and $C_{YY}(t) = \sigma^2_{y,0}[1 - e^{-2\alpha_Y t} + \beta_{YX} f(t)]$, where $f(t) = \frac{1-e^{-2\alpha_Y t}}{1+m_{YX}} + \frac{4m_{YX}e^{-(\alpha_X+\alpha_Y)t}}{(1+m_{YX})(1-m_{YX})^2} - \frac{4m_{YX}e^{-2\alpha_Y t}}{(1+m_{YX})(1-m_{YX})^2} + \frac{m_{YX}(e^{-2\alpha_Y t}-e^{-2\alpha_X t})}{(1-m_{YX})^2}$. It can be shown that $f(t)$ is at most of the order of unity. Hence, if $\beta_{YX} \ll 1$, one can take $1 - \rho^2_{XY} \approx 1$ and $C_{YY}(t) \approx \sigma^2_{y,0}(1 - e^{-2\alpha_Y t})$ yielding $F^2_{X\to Y}(t) \approx \frac{\beta_{YX} m_{YX}(e^{-\alpha_Y t}-e^{-\alpha_X t})^2}{(1-m_{YX})^2(1-e^{-2\alpha_Y t})}$. For a particular case of $m_{YX} = 1$, one finds $F^2_{X\to Y}(t) \approx \frac{\beta_{YX}\alpha^2_X t^2 e^{-2\alpha_X t}}{1-e^{-2\alpha_X t}}$ by taking the respective limit $\alpha_X \to \alpha_Y$.

Recalling Eq. (12), at $c_{XY} = 0$ one has $S_{X\to Y} = S^{\rm uni}_{X\to Y} = \beta_{YX}/(1 + m_{YX})$. Hence, both $S_{X\to Y}$ and $F^2_{X\to Y}(t)$ are proportional to β_{YX} revealing a simple relation

$$S_{X\to Y} = S^{\rm uni}_{X\to Y} = k_{YX,t} F^2_{X\to Y}(t), \tag{13}$$

where the proportionality coefficient

$$k_{YX,t} = \frac{(1 - m_{YX})^2(1 - e^{-2m_{YX}\alpha_X t})}{m_{YX}(1 + m_{YX})(e^{-m_{YX}\alpha_X t} - e^{-\alpha_X t})^2} \tag{14}$$

depends on the relaxation times of the systems and does not depend on the coupling parameter β_{YX} for the case of weak couplings considered. For the short-term effect over an interval $\Delta t \ll \min(\tau_X, \tau_Y)$, it holds true that $F^2_{X\to Y}(\Delta t) \approx \beta_{YX}\alpha_X \Delta t/2$ and, hence,

$$S_{X\to Y} = S^{\rm uni}_{X\to Y} \approx (\bar\tau/\Delta t) F^2_{X\to Y}(\Delta t), \tag{15}$$

i.e., $k_{YX,\Delta t} \approx \bar\tau/\Delta t \gg 1$. One-step-ahead PI $G'_{X\to Y}$ for such a small sampling interval Δt is typically close to $F^2_{X\to Y}(\Delta t)$ as confirmed by the numerical examples below. Then, knowing the mean relaxation time $\bar\tau$, one can estimate the long-term effect $S_{X\to Y}$ through multiplication of $G'_{X\to Y}$ by the respective sufficiently large number $k_{YX,\Delta t}$. For example, for many climatic time series, that multiplier should often be of the order of 10, and typical small values of the one-step-ahead PI for monthly data (e.g., 1–2%) [12,13] may imply rather considerable long-term contributions of the coupling to the observed dynamics (e.g., 10–20% in terms of variance). This is an important conclusion that helps to avoid underestimation of small numerical values of PIs in practice.

To consider lower sampling frequencies, we denote with a prime the nondimensional time $t' = t/\min(\tau_X, \tau_Y)$ and note that $F^2_{X\to Y}(t) = S_{X\to Y}/k_{YX,t}$. The coefficient $1/k_{YX,t}$ depends on t' and m_{YX} [Fig. 1(a)] and its maximal value corresponds to the maximal short-term effect $F_{X\to Y,\max}$. At $m_{YX} \ll 1$ (the driving system X is much faster than Y), one gets from

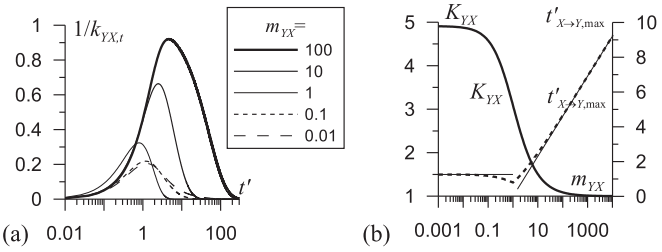

FIG. 1. Relations between short-term and long-term causal effects for the system (8) at $c_{XY} = 0$ and $\Gamma_{XX} = 2\alpha_X$ and $\Gamma_{YY} = 2\alpha_Y$ at weak couplings $\beta_{YX} \ll 1$: (a) the ratio $F^2_{X\to Y}(t)/S_{X\to Y}$ vs $t' = t/\min(\tau_X, \tau_Y)$; (b) the coefficient $K_{YX} = S_{X\to Y}/F^2_{X\to Y,\max}$ (the thick solid line) and the normalized time $t'_{X\to Y,\max}$ of the maximal short-term effect (the dashed line) together with its approximations $t'_{X\to Y,\max} = 1.26$ for smaller m_{YX} and $t'_{X\to Y,\max} = \ln m_{YX}$ for larger m_{YX} (the thin solid lines) vs the ratio of relaxation times m_{YX}.

(14) that the maximum effect time is $t'_{X\to Y,\max} \approx 1.4$, i.e., $t_{X\to Y,\max} \approx 1.4\tau_X$, which is a bit greater than the smallest relaxation time [Fig. 1(b)]. At $m_{YX} \gg 1$ (the driving system X is much slower), one gets $t'_{X\to Y,\max} \approx \ln m_{YX}$, i.e., $t_{X\to Y,\max} \approx \tau_Y \ln m_{YX}$ is greater than the smallest relaxation time only by the factor of $\ln m_{YX}$. In general, one gets

$$S_{X\to Y} = S^{\rm uni}_{X\to Y} = K_{YX} F^2_{X\to Y,\max}, \tag{16}$$

where the coefficient $K_{YX} = \min_t[k_{YX,t}]$ depends only on m_{YX}. In Fig. 1(b), one can see that the value of K_{YX} varies from 1 (for $m_{YX} \gg 1$) to approximately 5 (for $m_{YX} \ll 1$). Hence, even for sufficiently sparse samplings, the long-term effect is at least several times as large as the normalized PI value, except for a specific situation when the driving system X is much slower than the driven one and the prediction interval Δt is close to $\tau_Y \ln m_{YX}$.

Let us check the validity of the obtained relationships in a wide range of β_{YX} for three characteristic values of m_{YX}: $m_{YX} = 1$, $m_{YX} = 0.1$, and $m_{YX} = 10$. In the first case, the quantity $F_{X\to Y}(t)$ reaches its maximum at $t'_{X\to Y,\max} \approx 0.82$ and one gets $S_{X\to Y} \approx 3.1 F^2_{X\to Y,\max}$ [Fig. 1(b)]. This relationship is valid for moderately large couplings, as illustrated in Fig. 2(a): the relative discrepancy between the values $S_{X\to Y}$ (the thick solid line) and $3.1 F^2_{X\to Y}$ (the thin solid line) is less than 20% up to $S_{X\to Y} \approx 0.2$. The dashed lines in Fig. 2(a) show $F^2_{X\to Y}(t)$ at fixed t's multiplied by the corresponding coefficients (14). Note that the time $t' = 0.1$ may be regarded as small compared to unity, i.e., one may apply (15) and use $k_{YX,t} = 10$. Indeed, $t' = 0.1$ corresponds to the value of $k_{YX,t} = 11.1$ according to Eq. (14), which is close to the above rough approximation $k_{YX,t} = 10$. At $t' = 0.2$ an accurate value of $k_{YX,t} = 6.25$ obtained from Eq. (14) differs stronger (by 25%) from the respective approximation $k_{YX,t} = 5$. In the case of $t' = 1/3$, which is still smaller than the maximum time $t'_{X\to Y,\max} = 0.82$, one has $k_{YX,t} = 4.25$, which differs almost by 50% from its rough approximation of $k_{YX,t} = 3$. Thus, in practice the sampling interval Δt equal to 1/5 of the characteristic time scale should be considered as a boundary case between the high sampling frequency situation where Eq. (15) works well, and the lower sampling frequency case where only the more general relationships (13) and (14) are

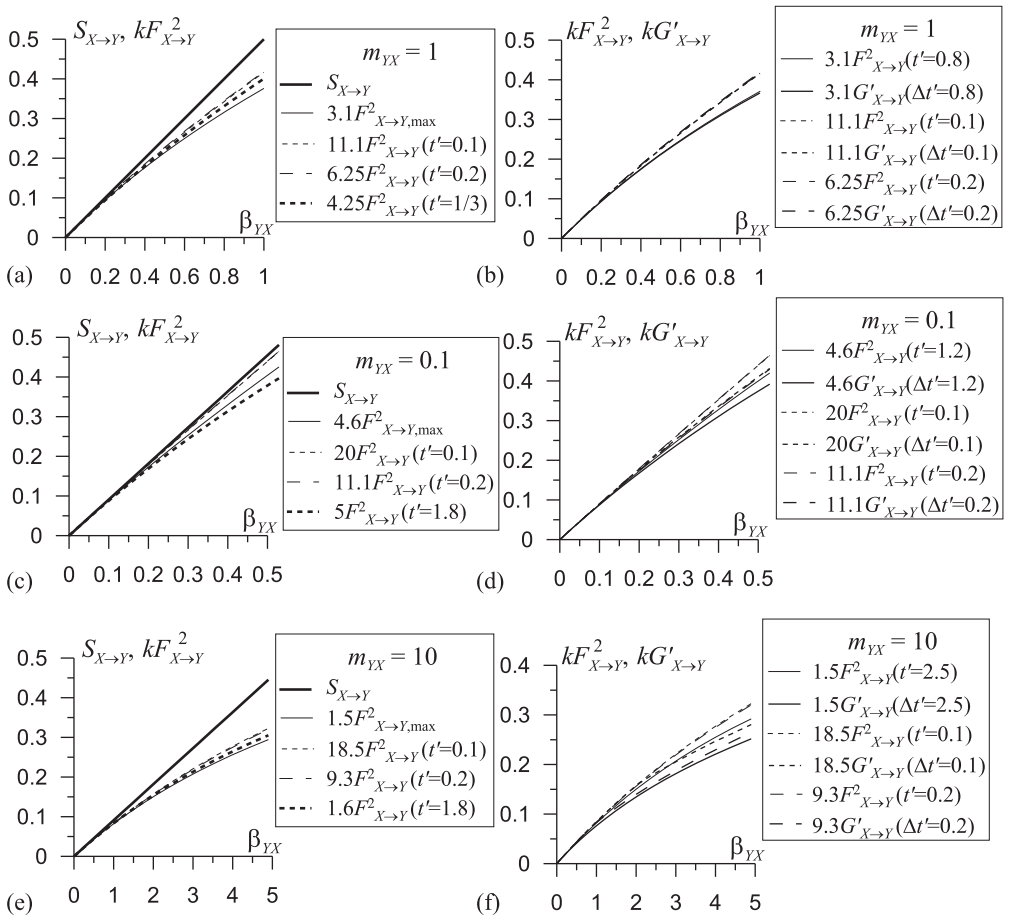

FIG. 2. Long-term and short-term causal effects for the system (8) at $c_{XY} = 0$ and $\Gamma_{XX} = 2\alpha_X$ and $\Gamma_{YY} = 2\alpha_Y$ vs the normalized coupling parameter, which is varied due to varying c_{YX}. The left column compares $S_{X\to Y}$ to the scaled fixed-time and maximal short-term effects (indicated by the respective lines described in the legends). The right one compares Granger causality at various sampling intervals and the respective fixed-time causal effects: $\alpha_X = \alpha_Y = 1$ (a) and (b); $\alpha_X = 10$, $\alpha_Y = 1$ (c) and (d); $\alpha_X = 1$, $\alpha_Y = 10$ (e) and (f).

to be used. As for the correspondence between $F^2_{X\to Y}$ and $G'_{X\to Y}$, it is quite precise and the respective plots in Fig. 2(b) just coincide for any coupling strength and sampling interval considered.

If a fast system drives a slow one ($\alpha_X \gg \alpha_Y, m_{YX} \ll 1$), one gets $S_{X\to Y} \approx \beta_{YX}$ and $F^2_{X\to Y}(t) \approx \frac{\beta_{YX} m_{YX}(e^{-\alpha_Y t} - e^{-\alpha_X t})^2}{1-e^{-2\alpha_Y t}}$. One may roughly take that $t_{X\to Y,\max} \approx \tau_X$ if the two relaxation times differ only by one or two orders of magnitude. Then, one gets $F^2_{X\to Y,\max} \approx \beta_{YX}(1-1/e)^2/2 \approx 0.2\beta_{YX}$ so that $S_{X\to Y} \approx 5F^2_{X\to Y,\max}$, i.e., $K_{YX} \approx 5$. The precise solution for weak couplings [Fig. 1(b)] gives the asymptotic values of $t_{X\to Y,\max} = 1.26\tau_X$ and $K_{YX} = 4.9$. Thus, at $m_{YX} = 0.1$ one has $t_{X\to Y,\max} = 1.26\tau_X$ and $K_{YX} = 4.6$, which is illustrated in Figs. 2(c) and 2(d), where $\tau_X = 0.1$, $\tau_Y = 1$, and $\bar{\tau} = 0.18$. One observes the correspondence between $S_{X\to Y}$ and the scaled short-term effects in Fig. 2(c) similar to (and even a bit better than) that in Fig. 2(a). The correspondence between PIs and the short-term effects in Fig. 2(d) is a bit worse than that in Fig. 2(b), but also quite precise: the relative difference is less than 5% in the entire range of the coupling parameter.

In the opposite case of $\alpha_Y \gg \alpha_X$, one gets $S_{X\to Y} \approx \beta_{YX}/m_{YX}$ and $F^2_{X\to Y,\max} \approx \beta_{YX}/m_{YX}$ at $t'_{X\to Y,\max} \approx \ln m_{YX}$, so that $K_{YX} \approx 1$. At moderately large $m_{YX} = 10$ [Figs. 2(e) and 2(f)], one gets $S_{X\to Y} \approx 0.09\beta_{YX}$ and $F^2_{X\to Y,\max} \approx 0.06\beta_{YX}$ at $t_{X\to Y,\max} = 2.3\tau_Y$, so that $K_{YX} \approx 1.5$. Figure 2(e) shows the correspondence between $S_{X\to Y}$ and the scaled short-term effects similar to (a bit worse than) that in Fig. 2(a). The correspondence between PIs and the short-term effects in Fig. 2(f) is a bit worse than that in Fig. 2(b) but also quite good: the relative difference is less than 10% up to the values corresponding to $S_{X\to Y} \approx 0.2$.

To summarize, knowing PIs and relaxation times and using the above relationships (13)–(16) along with Fig. 1(b), one can compute the long-term effect $S_{X\to Y}$ with a relative error less than 20% if the resulting value of $S_{X\to Y}$ is less than ≈0.2. If the resulting value exceeds 0.2, it may be overestimated so that one should more carefully conclude that $S_{X\to Y} \approx 0.2$ or greater. The simplified formula (15) is applicable if the sampling interval is ≈5 times less than the mean relaxation time or smaller.

C. Bidirectional coupling

The processes x and y in Eqs. (8) are stationary if and only if $\alpha_X\alpha_Y - c_{XY}c_{YX} > 0$. Hence, the denominator in Eq. (11) is positive while $S_{X\to Y}$ is positive or negative depending on the sign of the expression $c^2_{YX}\sigma^2_{x,0} + c_{XY}c_{YX}\sigma^2_{y,0}$. This situation

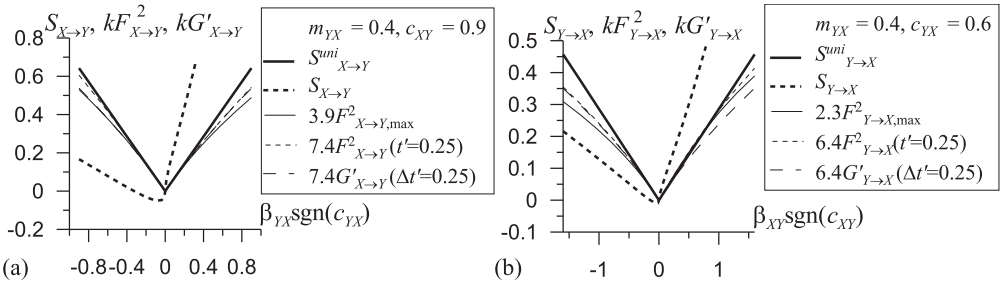

FIG. 3. Short-term and long-term causal effects for the system (8) with $\alpha_X = 2.5$, $\Gamma_{XX} = 2\alpha_X$, $\alpha_Y = 1$, $\Gamma_{YY} = 2\alpha_Y$ vs signed β_{YX} at $c_{XY} = 0.9$ (a) and vs signed β_{XY} at $c_{YX} = 0.6$ (b).

differs from the unidirectional case in which $S_{X\to Y}$ is always positive. As for the unidirectional effect $S^{\mathrm{uni}}_{X\to Y}$, it is the same (12) in both cases by its very definition. Symmetrically, the opposite effect reads $S^{\mathrm{uni}}_{Y\to X} = \frac{\beta_{XY}}{1+m_{XY}}$, where $m_{XY} = \frac{\alpha_X}{\alpha_Y}$ and $\beta_{XY} = \frac{c^2_{XY}\Gamma_{YY}}{\alpha^2_Y\Gamma_{XX}}$.

Let us introduce an additional nondimensional parameter $r = \frac{c_{XY}c_{YX}}{\alpha_X\alpha_Y}$, which characterizes the "total interaction intensity" relative to the "total relaxation intensity." It is easy to see that $r^2 = \beta_{YX}\beta_{XY}$. The value of r is less than unity for stationary processes, and the sign of r is given by $\mathrm{sgn}(r) = \mathrm{sgn}(c_{XY}c_{YX})$. By transforming Eq. (11), one gets $S_{X\to Y} = \frac{S^{\mathrm{uni}}_{X\to Y}+\Delta S_{X\to Y}}{1-r}$, where $\Delta S_{X\to Y} = \frac{r}{1+m_{YX}}$ can be interpreted as an additive correction to the unidirectional effect $X \to Y$ due to the presence of nonzero coupling $Y \to X$. Hence, a nonzero coupling $Y \to X$ for negative r (i.e., for c_{XY} and c_{YX} of different signs) gives $S_{X\to Y} < S^{\mathrm{uni}}_{X\to Y}$ both due to the negative addendum $\Delta S_{X\to Y}$ and to the denominator $(1-r) > 1$. Moreover, $S_{X\to Y}$ becomes even negative (the variance of y decreases in the coupled case as compared to the free variance) if $c_{YX}c_{XY} < 0$ and $|c_{YX}|\sigma^2_{x,0} < |c_{XY}|\sigma^2_{y,0}$, i.e., if the coupling term in the opposite direction $Y \to X$ is large enough in absolute value. If the coupling coefficients are of the same sign, one observes a greater long-term effect $S_{X\to Y} > S^{\mathrm{uni}}_{X\to Y}$ both due to positive $\Delta S_{X\to Y}$ and to the denominator $(1-r) < 1$. Such a complicated dependence of $S_{X\to Y}$ on the coupling parameters is shown in Fig. 3, where one can see that the simple proportionality between $S_{X\to Y}$ and short-term effects is no longer valid in the entire range of coupling parameter values.

The linear relationships (13), (15), and (16) are still approximately valid for the unidirectional effects $S^{\mathrm{uni}}_{X\to Y}$ and $S^{\mathrm{uni}}_{Y\to X}$. Indeed, consider the system (8) with bidirectional coupling and damping terms $\alpha_X = 2.5$ and $\alpha_Y = 1$ as an example (Fig. 3). These values are selected so as to mimic the correlation properties of the climatic processes analyzed in Sec. VI, though the results are qualitatively similar for any relaxation times. Since $\bar{\tau} \approx 0.57$, for $\Delta t = 0.1$ (i.e., $\Delta t' = 0.25$) rough estimates $S^{\mathrm{uni}}_{X\to Y} \approx 5.7G'_{X\to Y}$ and $S^{\mathrm{uni}}_{Y\to X} \approx 5.7G'_{Y\to X}$ follow from Eq. (15). Determining $k_{X\to Y,\Delta t}$ and $k_{Y\to X,\Delta t}$ more precisely (14), one gets $S^{\mathrm{uni}}_{X\to Y} \approx 7.4G'_{X\to Y}$ and $S^{\mathrm{uni}}_{Y\to X} \approx 6.4G'_{X\to Y}$. These relationships are valid to good accuracy at least up to the values of $S^{\mathrm{uni}} \approx 0.2$ again (Fig. 3). Hence, the unidirectional long-term effects can be computed via the linear formula (13) even from PIs estimated for bidirectionally coupled systems. As for the full long-term effects, one can relate $S_{X\to Y}$ to PIs based on the above relationships between $S_{X\to Y}$ and $S^{\mathrm{uni}}_{X\to Y}$, but the resulting expressions are more cumbersome and depend on the signs of the coupling coefficients. They are not reported here.

D. Discussion of the theoretical results

What is most valuable is that we have shown a principal opportunity to relate such different manifestations of couplings as the above short-term and long-term effects. This is done for a concrete class of systems, even though they are widely encountered in theory and practice. A further analysis for broader classes of systems with richer sets of properties (rather than just relaxation times) is relevant and may reveal more complicated dependencies between the two types of coupling characteristics. However, such an analysis will be inevitably more difficult, which makes the simple, vivid, and rigorous results obtained for the systems (8) quite a useful reference point for understanding more complex relationships and their origin.

As for the practical value, the obtained simple expressions provide a concrete way of estimating the long-term effect on the basis of PI estimate through multiplication of $G'_{X\to Y}$ by the appropriate coefficients $k_{YX,\Delta t}$ or K_{YX}. Being strictly applicable to the linear overdamped oscillators (8), the obtained relationships can be reasonably accurate for a broad range of real-world processes, which is motivated as follows. Even in analysis of complex nonlinear processes, it may happen that for spatial and temporal scales of interest, it is sufficient to study a linearized version of the full nonlinear equations with stochastic terms, the so-called "stochastic forcing models" of Hasselmann [53], who discussed this reason for "reddening" of the power spectra of many climate processes. As a practical consequence of such observations, one often tests against the "red-noise model" (which is exactly an overdamped oscillator considered above) to assess the statistical significance of data analysis results, e.g., in cross-wavelet analysis [54] and many other studies. Furthermore, climate indices typically represent states of a broad region in the ocean or the atmosphere (implying spatial averaging) in terms of deviations from mean climatology (resembling perturbation analysis). These are the likely reasons why climate models of intermediate complexity often show that nonlinearity is not clearly manifest in the dynamics of spatiotemporal modes of variability [55]. As argued in the cited works, nonlinearity determines the spatial structure of such modes, while the temporal dynamics of their amplitudes (climate indices) may well be represented by stochastic linear equations. Thus, the linearity of the considered systems (8) may not be such a serious obstacle

for the applicability of the derived relationships to many natural processes. A more limiting factor is its low dimensionality, which means that each of the systems has only one characteristic time scale, namely the decay time of the autocorrelation function (ACF). Let us discuss using two mathematical examples how (i) higher dimensionality and (ii) nonlinearity of the systems under study limit the applicability of the derived relationships.

Higher-dimensional linear systems X and Y may exhibit other characteristic times, e.g., basic oscillation periods, along with the relaxation times. In particular, consider unidirectionally coupled dissipative linear oscillators X and Y represented by the equations $\dot{x}_1 = -\alpha x_1 + \omega x_2 + \xi_{x,1}(t)$, $\dot{x}_2 = -\alpha x_2 - \omega x_1 + \xi_{x,2}(t)$, $\dot{y}_1 = -\alpha y_1 + \omega y_2 + c_{YX} x_1 + \xi_{y,1}(t)$, and $\dot{y}_2 = -\alpha y_2 - \omega y_1 + \xi_{y,2}(t)$ with independent white noise of the same intensity and observables $u = x_1$ and $v = y_1$. In an uncoupled case, the observables exhibit ACFs given by $\exp(-\alpha t)\cos(\omega t)$. If $(\omega/\alpha)^2 \ll 1$, these oscillators are close to the overdamped oscillators, and it can be shown that Eqs. (13) and (14) are valid with a small relative error proportional to $(\omega/\alpha)^2$. This error may be quite large if $\omega/\alpha \gg 1$ when ACFs exhibit slowly decaying oscillations, which is easily recognized in practice. However, one can check numerically that Eqs. (13) and (14) are still reasonably accurate for intermediate cases in which ACFs just decay fast enough, i.e., relaxation dominates over oscillations and no more than a single oscillation is clearly seen in the ACF estimate (strongly dissipative oscillators). Then, one can fit an exponential function to the empirical ACF over several smallest time lags and use the resulting exponent as an estimate of the relaxation rate in the model (8). Such a case study is performed in Sec. VI with an AR model of climate processes. As for the parametrization of coupling used in Eq. (8), it reflects many real-world situations, especially when the variables x and y are of a different physical nature and represent small deviations from a basic regime; see, e.g., a description of the mutual effects of cloudiness and surface air temperature in Sec. II.3 of Ref. [30]. In more special cases, the coupling term can take the form $c_{YX}[x(t) - y(t)]$ or another one that can give somewhat different values of the coefficient relating short-term and long-term effects. Whenever available, *a priori* information about the form of coupling can be used to modify the relationships (13) and (14) similarly to the derivation of Sec. V B. However, the derived formulas based on the most parsimonious coupling function (8) seem to be most widely applicable.

As an example of nonlinear systems, consider stochastic quadratic maps $x_{n+1} = r x_n(1 - x_n) + \xi_{x,n}$, $y_{n+1} = r y_n(1 - y_n) + c_{YX} x_n + \xi_{y,n}$, where r is the "nonlinearity" parameter and ξ's are independent white noises with the variance σ_ξ^2. At small $r \ll 1$ and $\sigma_\xi \ll 1$, this is a discrete-time version of the overdamped oscillators (8): variance of x equals $\sigma_\xi^2/(1 - r^2)$ and would be zero in the absence of noise; a nonzero variance of y is also completely determined by the presence of the term $c_{YX} x_n + \xi_{y,n}$. By increasing r, one observes period-doubling bifurcations in both systems leading finally to chaotic regimes. Then, the amplitude of the y variations strongly exceeds $\sigma_\xi^2/(1 - r^2)$, being determined by the intrinsic nonlinear dynamics of y rather than by the small perturbation term $c_{YX} x_n + \xi_{y,n}$. The latter determines only a small part of the y variance [32], and the long-term effect $S_{X\to Y}$ is therefore small while the short-term effects may be quite large since they are measured by the ratio of $c_{YX} x_n$ to $\xi_{y,n}$. Then, the relationships (13) and (14) may no longer be valid. Such situations can be recognized in practice by strong signs of nonlinearity, in particular by much better short-term predictions of nonlinear empirical AR models as compared to linear AR models. One needs then *a priori* information about underlying mechanisms and a nonlinear model fitted to the data (e.g., via Bayesian inference [56] or other techniques [6]) to quantify long-term effects, which is a subject of future research. However, if the nonlinearity is sufficiently weak, then the relationships (13) and (14) are applicable, as can be checked numerically, e.g., for the case of reasonably small r and σ_ξ in the above example. Such cases are to be diagnosed in practice by weak signs of nonlinearity, e.g., when predictions of nonlinear AR models are not essentially superior over linear ones. The latter is the case for many time series characterizing large-scale climate processes. In particular, the climatic example below seems to represent strongly damped oscillations without strong signs of nonlinearity, which is evidence of the applicability of the above relationships for long-term effect estimation. Independently of this argument, the empirical bivariate AR model (1) of those climatic processes appears higher-dimensional than the system (8), so by analyzing long-term effects in that model, we provide a case study of the validity of the relationships (13) and (14) beyond overdamped oscillators.

VI. APPLICATION TO CLIMATIC TIME SERIES

Major climatic processes of global importance are related to the natural quasicyclic phenomena of El − Niño–Southern Oscillation (ENSO) and Atlantic Multidecadal Oscillation (AMO). In particular, significant interannual and interdecadal variations in global surface temperature are related to these modes of climate variability [57–59]. ENSO processes are characterized by strong variations of surface temperature in the equatorial zone of the Pacific Ocean with typical intervals of 2–8 years and a spectral maximum at 4–5 years. El − Niño phenomena display also interdecadal variations and longer-term changes [60,61]. The AMO index represents variations in the mean North Atlantic (NA) sea surface temperature (SST). It got its name due to the presence of approximately 60-year periodicity [62,63]. Such a slow variability is regarded as a manifestation of changes in deep ocean circulation (Atlantic meridional overturning circulation), and it is currently considered as a possible cause of the recent slowdown of global warming [59,64]. At the same time, decadal and intradecadal time scales of variability are also present in the NA SST variations represented by the AMO index [65]. For a better understanding of global climate variations, it is important to reveal how its possible drivers interact with each other [66], and, in particular, to characterize the mutual influence of ENSO and NA SST variations at different time scales. For the latter, Granger causality along with an estimation of the long-term effect should provide useful hints.

A. Data and their ACFs

We estimate PIs and the long-term causal effects between North Atlantic SST variations (the system X') and equatorial

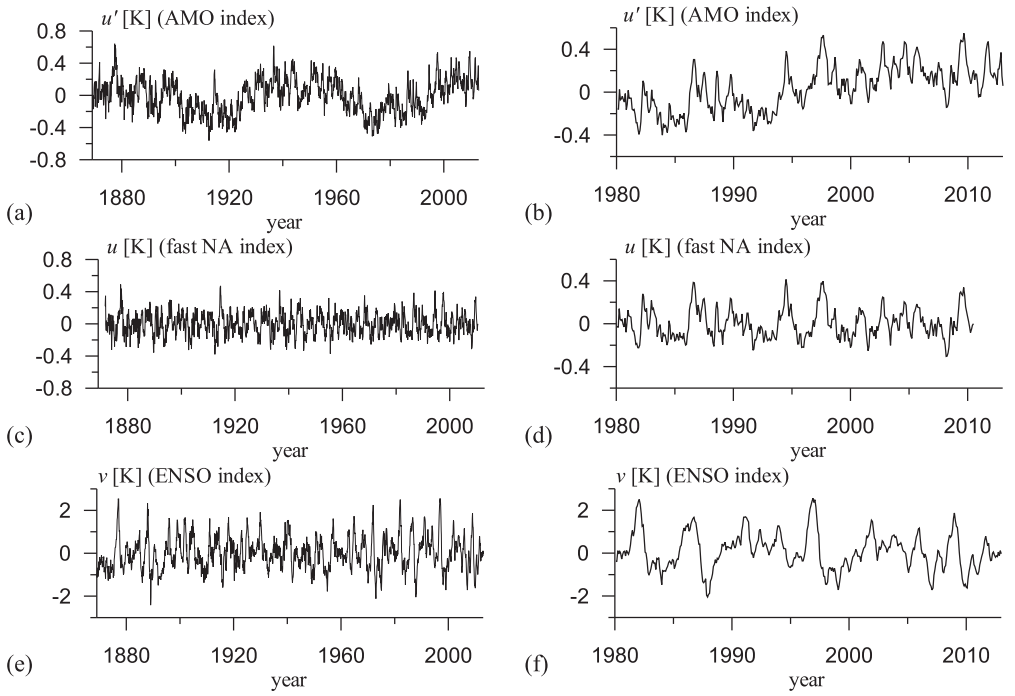

FIG. 4. Time series of the climatic indices under study. The right panels are magnified segments (the most recent 30 years) of the corresponding left panels. AMO index (a) and (b); "fast NA" index, which is a high-pass filtered AMO signal (c) and (d); ENSO index Nino-3.4 (e) and (f).

Pacific SST variations (the system Y) from the time series of monthly indices of AMO and ENSO over the period 1870–2013, covering 144 full years. The AMO index is the NA SST over 0–70°N, which is denoted u' and shown in Figs. 4(a) and 4(b). As the ENSO index, we take the SST in the Nino-3.4 region 5°S–5°N, 150°W–90°W, which is denoted v and shown in Figs. 4(e) and 4(f). Of separate interest is an analysis of a faster component in the NA SST variations (the system X) characterizing interannual variability with time scales close to the basic time scales of the ENSO dynamics. For that, we high-pass filter the AMO index $u'(t)$ by subtracting its 5-year running mean, and we call the resulting quantity $u(t)$ the "fast NA" index [Figs. 4(c) and 4(d)]. By considering a 30-year segment of the whole period [Figs. 4(b) and 4(d)], one can see that the u signal captures the basic features of the original u' signal, except for the slow (60-year) variability, which is clearly seen in Fig. 4(a) and absent in Fig. 4(c). Moreover, the analysis of couplings between X and Y should provide conclusions with a better statistical justification than that for the pair X' and Y because the available period 1870–2013 covers many characteristic time scales of u and v, which is not the case for u'.

Empirical ACFs for all signals are shown in Figs. 5(a) and 5(b): the ACF for the u signal [Fig. 5(a), circles] decays over time lags of 5–6 months exponentially at a rate of 0.25 month^{-1} [Fig. 5(a), thin solid line], which corresponds to the relaxation time $\tau_X = 4$ months. Its further behavior is better described by a damped cosine function [Fig. 5(a), dashed line] whose estimate is less reliable due to smaller ACF values at larger time lags, and which is nevertheless inappropriate for small lags. ACF for the original AMO index u' [Fig. 5(a), crosses] is overall slowly decaying, so its estimate is not reliable. Still, fitting an exponential function up to time lags of 3–4 months gives a decay rate of 0.09 month^{-1} and $\tau_{X'} = 11$ months. The ACF for the ENSO index up to time lags of four months is well described by an exponent 0.1 month^{-1} [Fig. 5(b), thin solid line] corresponding to the relaxation time $\tau_Y = 10$ months, while a damped cosine function is a better description only for greater time lags.

B. Estimation techniques

Granger causality estimation is performed according to the well-established procedure described in detail in Ref. [13]. Namely, to estimate $G_{X\to Y}$ we fit univariate and bivariate AR models (1) to the time series $\{u_n, v_n\}$ using the ordinary least-squares technique. An optimal model order d_Y is selected by minimizing Schwarz' information criterion [67]. Then, we find PIs for different d_{YX} and assess the statistical significance (p-level) of the PI positivity via Fisher's F-test [48]. Final d_{YX} is selected by minimizing the Bonferroni corrected (i.e., accounting for multiple testing with various d_{YX}) statistical significance level $p_{\min} = \min_{d_{YX}\geqslant 1}\{d_{YX}\, p\}$. Everything is similar for the opposite direction $G_{Y\to X}$. To validate all the AR models used, we check the δ-correlatedness of the residual errors by calculating their ACFs [47]. The similarity of their histograms to normal distributions is also checked, but it is not as important.

To estimate the long-term effect from a time series $\{u_n, v_n\}$, we use two procedures. The first one is a direct estimation (Sec. IV) where the bivariate AR model (1) obtained from Granger causality estimation is used as a proxy for the processes under study. Namely, we assume that "switching the coupling $X \to Y$ off" corresponds to zeroing all the

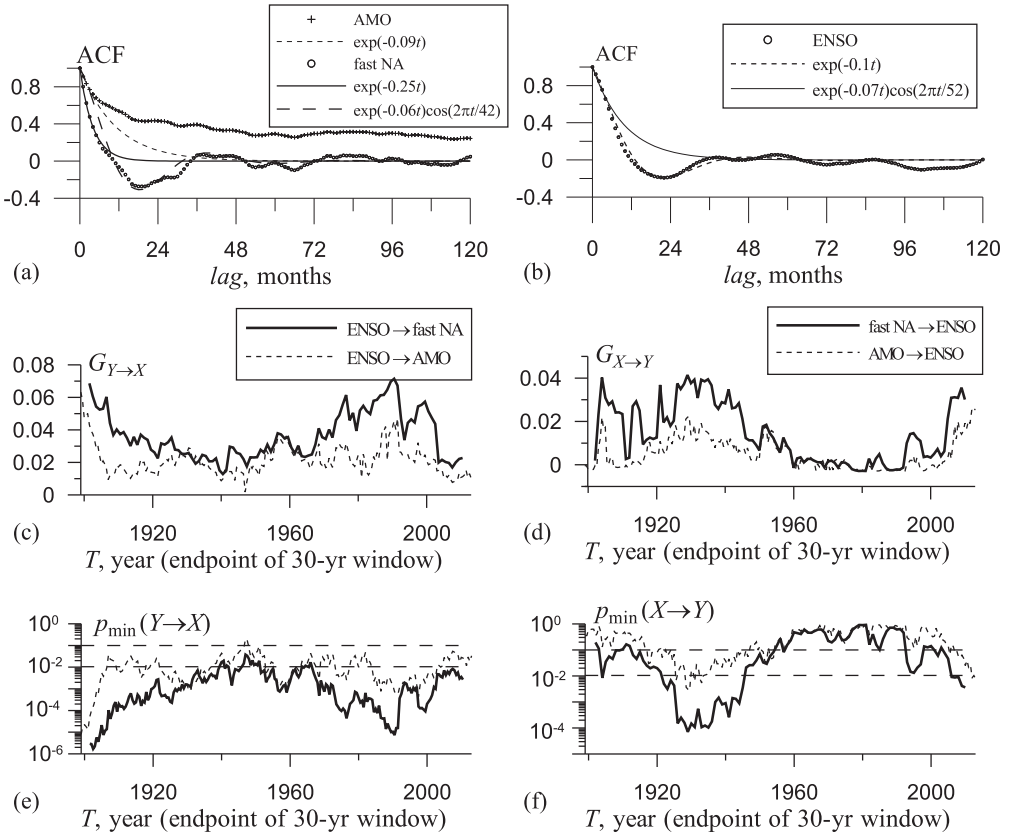

FIG. 5. ACF and Granger causality estimates for the climatic time series: ACF functions and their fits (a) and (b); PIs in a 30-year moving window $[T-30,T]$ vs T (c) and (d). Pointwise significance levels for each window: the dashed lines show the level of 0.01, which corresponds to the final (Bonferroni corrected) significance level of 0.05, and the level of 0.1, which corresponds to "something close to a significant result" (e) and (f).

coefficients $b_{v,k}$ in Eqs. (1) with all other parameters unchanged. Thereby, we find the variance of v in the model at zero and nonzero couplings, and we compute $S^{\text{uni}}_{X\to Y}$ and $S_{X\to Y}$. Let us call the latter "direct estimates." Since the validity of such extrapolation is not always assured, independent estimates are valuable and we use the second procedure based on the PI estimates, the relationships (13) and (14), and ACF decay times estimated above. Let us call them "PI-based estimates." In this case, we extrapolate the relationships (13) and (14) derived for overdamped oscillators to the processes under study, which can only be approximated to a certain accuracy in such a form. However, due to the simplicity of (13) and (14), one may expect them to be more robust (Sec. V D) than the AR model extrapolation. For the fast NA and ENSO indices, we take the relaxation times $\tau_X = 4$ and $\tau_Y = 10$ months and the corresponding coefficients $k_{XY,\Delta t}$ and $k_{YX,\Delta t}$ from Eq. (14). For the sampling interval $\Delta t = 1$ month, the latter are equal to $k_{YX,\Delta t} = 7.4$ and $k_{XY,\Delta t} = 6.4$, which are close to the rough guess $\bar{\tau}/\Delta t = 5.7$ from Eq. (15). For the original AMO and ENSO indices, we take $\tau_{X'} = 11$ months and $k_{YX,\Delta t} = k_{XY,\Delta t} = 11$, which are close to $\bar{\tau}/\Delta t \approx 10.5$.

As for the full long-term effects $S_{X\to Y}$ and $S_{Y\to X}$, we present only their direct estimates based on the extrapolation of the bivariate AR model (1) since their relationships with PIs in the case of bidirectionally coupled processes seem to be less robust due to their greater complexity, and knowledge is required of the signs of the coupling coefficients (Sec. IV).

C. Estimation results for the entire time interval 1870–2013

Optimal individual AR models over the entire period 1870–2013 are achieved for the fast NA index at $d_X = 1$ giving the individual prediction error $\sigma^2_{u,\text{ind}}/\text{var}[u] = 0.36$ and for the ENSO index at $d_Y = 6$ giving $\sigma^2_{v,\text{ind}}/\text{var}[v] = 0.14$. The latter model obtained from a shorter time series has already been analyzed in Ref. [13], where it has been found that the corresponding residual errors are δ-correlated and their distribution is overall not strongly different from Gaussian. In particular, it does not exhibit any signs of heavy tails or multimodality. Nonlinear models have appeared inferior to the linear AR model according to Schwarz' criterion. Those conclusions are confirmed here. Similar validation results are obtained for the AR model obtained for the fast NA index and for the bivariate AR models. Due to the δ-correlatedness of the residual errors, these AR models can adequately reproduce variances and ACFs of the processes under study. Thus, the models are validated according to the standard tests. In assessing "ENSO → fast NA" coupling, an optimal joint model is achieved at $d_{XY} = 2$ with $G_{Y\to X} = 0.033$ significant at $p_{\min} < 10^{-11}$, i.e., the influence is detected confidently. The opposite "fast NA → ENSO" coupling appears weaker but is still valid: An optimal $d_{YX} = 10$ gives $G_{X\to Y} = 0.015$ significant at $p_{\min} < 0.002$.

Direct estimates of the unidirectional long-term effects appear equal to $S^{\text{uni}}_{X\to Y} = 0.12$ and $S^{\text{uni}}_{Y\to X} = 0.17$, i.e.,

"ENSO → fast NA" coupling is stronger than the opposite one with respect to the long-term effects as well. According to the PI-based estimation, one gets $S^{\text{uni}}_{X\to Y} = 0.11$ (very good agreement with the direct estimates) and $S^{\text{uni}}_{Y\to X} = 0.22$ (reasonably good agreement). Concerning the full long-term effects, their direct estimates read $S_{X\to Y} = 0.13$ and $S_{Y\to X} = 0.17$, which are very close to the unidirectional effects. We note that for PIs of the order of 1.5% and 3.3% we get the long-term effects of the order of 11–13% and 17–22%. Hence, the observed mutual influences of the two processes are quite considerable with respect to their stationary variances, being of the order of 10%, contrary to the order of 1% in terms of PIs. This quantitative information is gained due to the analysis of the long-term causal effects, and it would not be accessible with the Granger causality analysis alone. In addition, it is interesting that ENSO does not appear to be just a driver, as inferred in many studies [12,58], but it is considerably influenced by the NA process in turn.

For the AMO index, one gets $d_{X'} = 1$ and $\sigma^2_{u',\text{ind}}/\text{var}[u'] = 0.17$. PI in the "ENSO → AMO" direction is similar to the above case at $d_{X'Y} = 2$ with $G_{Y\to X'} = 0.015$ significant at $p_{\min} < 10^{-6}$. For the opposite direction, one gets $d_{YX'} = 1$ with $G_{X'\to Y} = 0.0011$ significant only at $p_{\min} < 0.09$, i.e., one hardly detects the "AMO → ENSO" influence. It may be that the slow AMO variability masks the interaction between interannual components of the NA and ENSO processes. Direct estimates of the long-term effects are $S^{\text{uni}}_{X'\to Y} = 0.01$ and $S^{\text{uni}}_{Y\to X'} = 0.13$, while the PI-based estimates $S^{\text{uni}}_{X'\to Y} = 0.012$ and $S^{\text{uni}}_{Y\to X'} = 0.17$. This is again quite good agreement. The full long-term effects $S_{X'\to Y} = 0.0014$ and $S_{Y\to X'} = 0.09$ appear smaller than the unidirectional effects, contrary to the "fast NA-ENSO" analysis.

Apart from a discussion of the adequacy of the AR models or the overdamped oscillators model for the processes under study, we note that a good agreement between the two long-term effect estimation techniques evidences that the relationships (13) and (14) are quite accurate for the bivariate AR processes (1), which are characterized by higher-dimensional state spaces than the overdamped oscillators (8). Hence, we have demonstrated an example confirming the good accuracy of the relationships (13) and (14) for strongly dissipative but not overdamped oscillators, whose ACFs just decay sufficiently fast.

D. Moving window analysis

To reveal any signs of temporal variations of coupling "strength," we have performed a moving window analysis in which all the estimates are computed separately for different time windows. The window length of 30 years appears to provide an optimal tradeoff between statistical reliability and temporal resolution of the results. This window length coincides with the usual length of a reference period in climate research [57]. Granger causality estimates for the pair "fast NA-ENSO" indices are shown in Figs. 5(c)–5(f) (solid lines) versus the end point T of the window. Optimal d_X varies between the windows from 1 to 2, d_Y from 1 to 5, d_{XY} from 1 to 3, and d_{YX} from 1 to 6. PI estimates and pointwise (i.e., separate for each window) significance levels show that the "ENSO → fast NA" PI is almost always statistically significant and on average greater than the opposite one. In particular, the "ENSO → fast NA" PI was large in the beginning of the period under study (1870–1910) and around the windows with T = 1980–1990 (i.e., over the period 1950–1990). It has exhibited a decreasing tendency during the past decade in terms of T. The "fast NA → ENSO" PI was maximal and significant around T = 1930–1940 (i.e., over the period 1900–1940). It has become significant again during the past decade in terms of T, and it has exhibited an increasing tendency. Moreover, the "fast NA → ENSO" PI even exceeds the opposite PI for the last windows corresponding to $T \approx$ 2005–2010 (i.e., the period 1975–2010). The middle of the 20th century is an interval of small couplings in both directions. Thus, we observe signs of a temporally varying coupling character similarly to ENSO–Indian monsoon interaction [13].

The PI-based and direct estimates of the unidirectional long-term effects for the "fast NA-ENSO" pair are shown in Figs. 6(a) and 6(b) (thin solid lines and dashed lines). Despite the fact that moving-window-based estimates are strongly influenced by statistical errors due to smaller data amounts, the two estimates appear to agree reasonably well, especially for the last windows T = 1990–2010, where the PIs are highly significant and the relaxation times of both processes are close to their estimates for the entire period 1870–2013. The maximal discrepancy between the two long-term effect estimates for the "ENSO → fast NA" direction is observed for T = 1935–1965, but this is exactly the period where the respective PIs are on the border of significance. Otherwise, the relative discrepancy between the two estimates is quite moderate, which further confirms the robustness of the obtained relationships (13) and (14). The long-term effect estimates reveal basically the same evolution of "coupling strength" as PIs, but they complement the observed values of PIs (no greater than 5–6%) with long-term coupling contributions to variance, which may reach 30–40%. The latter should be more cautiously bounded by 20% as discussed in Sec. V B, but it should still remain quite considerable. Hence, the couplings under study may well be quite important to sustain the basic characteristics of the observed dynamical regime rather than being secondary circumstances.

The full long-term effects [Figs. 6(a) and 6(b), thick solid lines] are typically less than the unidirectional ones due to negative coupling coefficients in the direction "fast NA → ENSO" and positive coupling coefficients in the opposite direction. Another interesting observation is that the "fast NA → ENSO" effect $S_{X\to Y}$ was often negative in the beginning of the period under study, but over the last windows with T = 2000–2010 it has become positive due to a combination of an increase of the unidirectional "fast NA → ENSO" effect $S^{\text{uni}}_{X\to Y}$ and a decrease of the opposite effect $S^{\text{uni}}_{Y\to X}$.

For the pair of original AMO-ENSO, $d_{X'}$ varies from 1 to 2, $d_{X'Y}$ from 1 to 3, and $d_{YX'}$ from 1 to 2. The temporal profiles of the PIs between AMO and ENSO are similar to those for the fast NA index [dashed lines in Figs. 5(c)–5(f)], but the "AMO-ENSO" mutual couplings are considerably weaker. Long-term effect estimates for the "AMO-ENSO" pair are also similar to those for the "fast NA-ENSO" pair [Figs. 6(c) and 6(d)], but all coupling estimates for "AMO-ENSO" are smaller and less significant. Other high-pass filtered versions

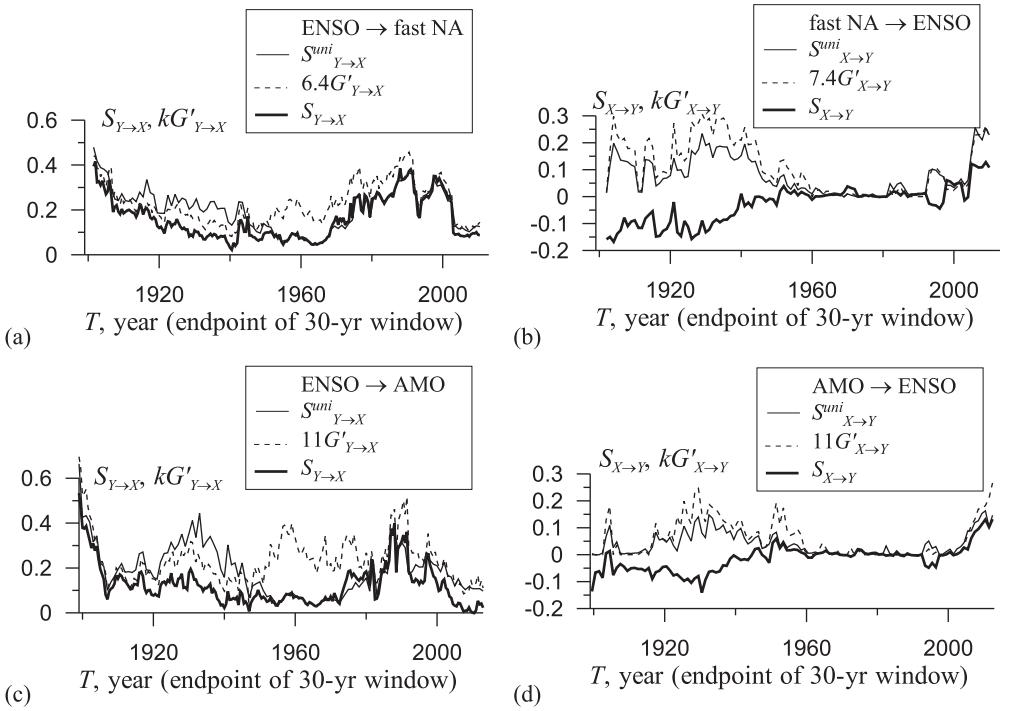

FIG. 6. The unidirectional long-term causal effects estimated from the AR model (thin solid lines) and from PIs (dashed lines) and full long-term effects estimated from the AR model (thick solid lines) for the pairs "fast NA-ENSO" (a) and (b) and "AMO-ENSO" (c) and (d).

of the AMO index (not reported here for brevity) have also been considered, e.g., subtraction of the 20-year running mean (instead of the 5-year mean) gives coupling estimates lying "in between" the respective values for the AMO and fast NA indices, closer to the latter case.

It is likely that the above nonzero coupling estimates for the "AMO-ENSO" pair are determined mainly by the interaction between ENSO and the faster component of NA SST variations. Still, couplings between ENSO and the slow 60-year NA mode might also be captured to a certain extent by the AR models used. To address the latter question, a systematic study of the coupling characteristics within various frequency bands is required. To provide a physical justification and understanding of the coupling character suggested by the results of the above analysis, further applications of the coupling estimation techniques to numerical atmospheric and oceanic circulation models seem relevant. This is beyond the scope of this paper, and we stress mainly the highly significant signs of mutual influences between intradecadal ENSO and NA SST variations presented in this section.

VII. CONCLUSIONS

As discussed in Ref. [28], there are many quantitative characteristics of causal couplings, and they can be classified into different families irreducible to each other in general. Some of those characteristics can be reliably estimated from data with existing techniques, but their numerical values lack a vivid physical interpretation (such as Granger causality). Others are clearly meaningful and of importance, but they are difficult to estimate in practice (such as the effects of couplings on stationary statistics). To make the entire field more ordered and the various coupling characteristics easier to interpret and to assess reliably, it is desirable to discover the relationships between them. This work contributes to solving this problem.

We have shown the existence of simple relationships between the short-term (on near future) and long-term (on stationary statistics) effects of causal couplings for a class of stochastic systems (linear overdamped oscillators). Namely, we have justified the fact that the normalized PI is an approximation of the short-term causal effect $F^2_{X\to Y}(t)$, which shows how strongly perturbations of a current state of X affect near future states of Y. As a representative of long-term causal effects, we have taken the quantity $S^{\mathrm{uni}}_{X\to Y}$, which shows a relative change in the variance of Y that occurs when a unidirectional coupling from X is switched on. Both $S^{\mathrm{uni}}_{X\to Y}$ and $F^2_{X\to Y}(t)$ may be measured in percent. Then, we have rigourously derived that for sufficiently weak couplings, these quantities are related as $S^{\mathrm{uni}}_{X\to Y} = k_{YX,t} F^2_{X\to Y}(t)$, where the proportionality coefficient is found as a function of the systems' relaxation times. The relationships are shown numerically to hold for moderately strong couplings up to $S^{\mathrm{uni}}_{X\to Y} \approx 20\%$. We have also argued that the relationships are valid to good accuracy for higher-dimensional linear systems if the ACFs of the observed signals decay exponentially, or, at least, if any oscillations of ACFs decay quickly, i.e., for strongly dissipative oscillators. In addition, the relationships are expected to be applicable to weakly nonlinear systems for which the nonlinear AR predictions are not essentially better than the linear ones.

In practice, the obtained formulas can make the traditional Granger causality characteristics (including those already reported in the literature) more informative by transforming the numerical values of PIs into long-term causal effects. Our theoretical study shows that small PI values should typically be increased several times to get the long-term effect (both in

percent), i.e., small PIs often correspond to quite a considerable long-term role of couplings. As an illustration, we have estimated couplings between large-scale climatic processes that reflect SST variations in equatorial Pacific and North Atlantic regions over the period 1870–2013. We have considered the AMO index, which reflects multidecadal variations in NA SST, and we focused on its high-pass filtered version representing interannual variations. Relying on the linear AR models (1) and the overdamped oscillators model (8), we have revealed evidence for the presence of a bidirectional coupling between the two processes, considerable long-term causal effects, and a stronger influence of "ENSO-to-NA" than "NA-to-ENSO" according to both short-term and long-term characteristics. For the entire period we have "ENSO → NA" PI about 3% while the long-term effect is $S^{\mathrm{uni}}_{Y\to X} \approx 17$–$22\%$. For the opposite direction, PI is about 1.5% and $S^{\mathrm{uni}}_{X\to Y} \approx 11$–$13\%$. Thus, the long-term effect estimation provides an alternative interpretation of the obtained small values of PIs suggesting that the detected couplings may be important in the long-term dynamics rather than being a small secondary effect. Similar results are obtained by the moving window analysis, which also suggests that the "ENSO → NA" effect was strong in the beginning of the period and near 1960–1990 and currently is decreasing, while the "NA → ENSO" influence was strong over the period of 1900–1940, then decreased, and currently is increasing again. The obtained quantitative estimates seem valuable for understanding the climate system behavior at interannual to multidecadal time scales, and they deserve further checks and studies with numerical climate models.

To deal with more general classes of systems, the rigorous results obtained here for overdamped oscillators can serve as a basis and reference point for deriving more general relationships between the short-term and long-term causal effects incorporating a richer set of dynamical characteristics. Such further studies seem quite relevant, and the obtained simple relationships may well retain their value even in those cases at least as heuristic tools.

ACKNOWLEDGMENTS

This work was supported by the Russian Science Foundation (Grant No. 14-12-00291). The climate data analysis of Sec. VI was also supported in part by the Government of the Russian Federation (Agreement No. 14.Z50.31.0033 with Institute of Applied Physics RAS) and the Russian Foundation for Basic Research (Grant No. 14-05-00639).

[1] M. Prokopenko and J. T. Lizier, Sci. Rep. **4**, 5394 (2014).
[2] M. Prokopenko, J. T. Lizier, and D. C. Price, Entropy **15**, 524 (2013).
[3] B. Kralemann, L. Cimponeriu, M. Rosenblum, A. Pikovsky, and R. Mrowka, Phys. Rev. E **76**, 055201 (2007); **77**, 066205 (2008).
[4] I. T. Tokuda, S. Jain, I. Z. Kiss, and J. L. Hudson, Phys. Rev. Lett. **99**, 064101 (2007).
[5] M. Pellicoro and S. Stramaglia, Physica A **389**, 4747 (2010); L. Angelini, M. de Tommaso, D. Marinazzo, L. Nitti, M. Pellicoro, and S. Stramaglia, Phys. Rev. E **81**, 037201 (2010).
[6] B. P. Bezruchko and D. A. Smirnov, *Extracting Knowledge from Time Series: An Introduction to Nonlinear Empirical Modeling* (Springer-Verlag, Berlin, 2010).
[7] J. Pearl, *Causality: Models, Reasoning, and Inference* (Cambridge University Press, Cambridge, 2000).
[8] Y.-C. Hung and C.-K. Hu, Phys. Rev. Lett. **101**, 244102 (2008).
[9] M. D. Prokhorov and V. I. Ponomarenko, Phys. Rev. E **72**, 016210 (2005); I. V. Sysoev, M. D. Prokhorov, V. I. Ponomarenko, and B. P. Bezruchko, *ibid.* **89**, 062911 (2014).
[10] G. Sugihara, R. May, H. Ye *et al.*, Science **338**, 496 (2012).
[11] W. Wang, B. T. Anderson, R. K. Kaufmann, and R. B. Myneni, J. Climate **17**, 4752 (2004); U. Triacca, Theor. Appl. Climatol. **81**, 133 (2005); T. J. Mosedale, D. B. Stephenson, M. Collins, and T. C. Mills, J. Climate **19**, 1182 (2006); E. Kodra, S. Chatterjee, and A. R. Ganguly, Theor. Appl. Climatol. **104**, 325 (2011).
[12] I. I. Mokhov and D. A. Smirnov, Geophys. Res. Lett. **33**, L03708 (2006); Izv. Atmos. Ocean. Phys. **44**, 263 (2008); Dokl. Earth Sci. **427**, 798 (2009); I. I. Mokhov, D. A. Smirnov, and A. A. Karpenko, *ibid.* **443**, 381 (2012).
[13] I. I. Mokhov, D. A. Smirnov, P. I. Nakonechny *et al.*, Geophys. Res. Lett. **38**, L00F04 (2011); Izv. Atmos. Ocean. Phys. **48**, 47 (2012).
[14] F. Donges, Y. Zou, N. Marwan, and J. Kurths, Europhys. Lett. **87**, 48007 (2009); J. H. Feldhoff, R. V. Donner, J. F. Donges, N. Marwan, and J. Kurths, Phys. Lett. A **376**, 3504 (2012).
[15] J. Runge, J. Heitzig, V. Petoukhov, and J. Kurths, Phys. Rev. Lett. **108**, 258701 (2012); J. Runge, J. Heitzig, N. Marwan, and J. Kurths, Phys. Rev. E **86**, 061121 (2012); J. Runge, J. Kurths, and V. Petoukhov, J. Climate **27**, 720 (2014).
[16] M. van der Mheen, H. A. Dijkstra, A. Gozolchiani *et al.*, Geophys. Res. Lett. **40**, 2714 (2013); Y. Wang, A. Gozolchiani, Y. Ashkenazy, Y. Berezin, O. Guez, and S. Havlin, Phys. Rev. Lett. **111**, 138501 (2013).
[17] M. Palus, Phys. Rev. Lett. **112**, 078702 (2014); Entropy **16**, 5263 (2014).
[18] S. J. Schiff, P. So, T. Chang, R. E. Burke, and T. Sauer, Phys. Rev. E **54**, 6708 (1996); J. Arnhold, K. Lehnertz, P. Grassberger, and C. E. Elger, Physica D **134**, 419 (1999); R. G. Andrzejak, A. Ledberg, G. Deco *et al.*, New J. Phys. **8**, 6 (2006); T. Kreuz, F. Mormann, R. G. Andrzejak *et al.*, Physica D **225**, 29 (2007); R. G. Andrzejak and T. Kreuz, Europhys. Lett. **96**, 50012 (2011).
[19] K. J. Friston, L. Harrison, and W. Penny, NeuroImage **19**, 1273 (2003); D. A. Pinotsis, R. J. Moran, and K. J. Friston, *ibid.* **59**, 1261 (2012).
[20] E. Pereda, R. Quian Quiroga, and J. Bhattacharya, Progr. Neurobiol. **77**, 1 (2005); J. Prusseit and K. Lehnertz, Phys. Rev. E **77**, 041914 (2008); B. Schelter, M. Winterhalder, M. Eichler *et al.*, J. Neurosci. Meth. **152**, 210 (2006); G. Nolte, A. Ziehe, V. V. Nikulin, A. Schlogl, N. Kramer, T. Brismar, and K. R. Muller, Phys. Rev. Lett. **100**, 234101 (2008); M. Wibral, B. Rahm, M. Rieder *et al.*, Prog. Biophys. Mol. Biol. **105**, 80 (2011); M. V. Sysoeva, E. Sitnikova, I. V. Sysoev *et al.*, J. Neurosci. Meth. **226**, 33 (2014); T. Stankovski, V. Ticcinelli, P. McClintock, and

A. Stefanovska, New J. Phys. **17**, 035002 (2015); A. K. Seth, A. B. Barrett, and L. Barnett, J. Neurosci. **35**, 3293 (2015).
[21] M. Staniek and K. Lehnertz, Phys. Rev. Lett. **100**, 158101 (2008); S. Stramaglia, G. R. Wu, M. Pellicoro, and D. Marinazzo, Phys. Rev. E **86**, 066211 (2012).
[22] I. Vlachos and D. Kugiumtzis, Phys. Rev. E **82**, 016207 (2010); D. Kugiumtzis, *ibid.* **87**, 062918 (2013); A. Papana, C. Kyrtsou, D. Kugiumtzis, and C. Diks, Entropy **15**, 2635 (2013).
[23] X. S. Liang, Phys. Rev. E **90**, 052150 (2014).
[24] H. Nalatore, N. Sasikumar, and G. Rangarajan, Phys. Rev. E **90**, 062127 (2014).
[25] H. Dickten and K. Lehnertz, Phys. Rev. E **90**, 062706 (2014).
[26] O. C. Guez, A. Gozolchiani, and S. Havlin, Phys. Rev. E **90**, 062814 (2014).
[27] J. M. McCracken and R. S. Weigel, Phys. Rev. E **90**, 062903 (2014).
[28] D. A. Smirnov, Phys. Rev. E **90**, 062921 (2014).
[29] J. Hlinka, D. Hartman, M. Vejmelka, D. Novotna, and M. Palus, Clim. Dyn. **42**, 1873 (2014); J. Hlinka, D. Hartman, N. Jajcay, M. Vejmelka, R. Donner, N. Marwan, J. Kurths, and M. Palus, Nonlin. Proc. Geophys. **21**, 451 (2014).
[30] I. I. Mokhov, *Diagnostics of the Climatic System Structure* (Gidrometeoizdat, St. Petersberg, (1993)) (in Russian).
[31] J. J. Tribbia and D. P. Baumhefner, Monthly Weather Review **132**, 703 (2004).
[32] D. A. Smirnov and I. I. Mokhov, Phys. Rev. E **80**, 016208 (2009).
[33] C. W. J. Granger, Econometrica **37**, 424 (1969).
[34] C. W. J. Granger, J. Econ. Dynam. Control **2**, 329 (1980).
[35] T. Schreiber, Phys. Rev. Lett. **85**, 461 (2000); K. Hlavackova-Schindler, M. Palus, M. Vejmelka, and J. Bhattacharya, Phys. Rep. **441**, 1 (2007).
[36] A. Porta, G. Baselli, F. Lombardi *et al.*, Biol. Cybern. **81**, 119 (1999); L. Faes, G. Nollo, and A. Porta, Phys. Rev. E **83**, 051112 (2011).
[37] M. Palus and A. Stefanovska, Phys. Rev. E **67**, 055201(R) (2003); M. Palus and M. Vejmelka, *ibid.* **75**, 056211 (2007); A. Bahraminasab, F. Ghasemi, A. Stefanovska, P. V. E. McClintock, and H. Kantz, Phys. Rev. Lett. **100**, 084101 (2008).
[38] C. A. Sims, Econometrica **39**, 545 (1971); H. Nalatore, M. Ding, and G. Rangarajan, Phys. Rev. E **75**, 031123 (2007); D. W. Hahs and S. D. Pethel, Phys. Rev. Lett. **107**, 128701 (2011); A. Seth, P. Chorley, and L. Barnett, NeuroImage **65**, 540 (2013).
[39] D. A. Smirnov and B. P. Bezruchko, Europhys. Lett. **100**, 10005 (2012).
[40] D. A. Smirnov, Phys. Rev. E **87**, 042917 (2013).
[41] A. Attanasio, A. Pasini, and U. Triacca, Atmos. Climate Sci. **3**, 514 (2013).
[42] I. I. Mokhov and D. A. Smirnov, Izv. Atmos. Ocean. Phys. **51**, 472 (2015).
[43] N. Ay and D. Polani, Adv. Complex Syst. **11**, 17 (2008).
[44] J. T. Lizier and M. Prokopenko, Eur. Phys. J. B **73**, 605 (2010).
[45] P. J. Webster, V. O. Magana, T. N. Palmer *et al.*, J. Geophys. Res. **103**, 14451 (1998).
[46] N. Ancona, D. Marinazzo, and S. Stramaglia, Phys. Rev. E **70**, 056221 (2004); D. Marinazzo, M. Pellicoro, and S. Stramaglia, Phys. Rev. Lett. **100**, 144103 (2008).
[47] G. E. P. Box and G. M. Jenkins, *Time Series Analysis. Forecasting and Control* (Holden-Day, San Francisco, 1970).
[48] G. A. F. Seber, *Linear Regression Analysis* (Wiley, New York, 1977).
[49] J. L. Lean and D. H. Rind, Geophys. Res. Lett. **35**, L18701 (2008); **36**, L15708 (2009).
[50] D. Mukhin, E. Loskutov, A. Mukhina, A. Feigin, I. Zaliapin, and M. Ghil, J. Climate **28**, 1940 (2015); D. Mukhin, D. Kondrashov, E. Loskutov, A. Gavrilov, A. Feigin, and M. Ghil, *ibid.* **28**, 1962 (2015).
[51] L. Barnett, A. B. Barrett, and A. K. Seth, Phys. Rev. Lett. **103**, 238701 (2009).
[52] D. W. Hahs and S. D. Pethel, Entropy **15**, 767 (2013).
[53] K. Hasselmann, Tellus **28**, 473 (1976).
[54] S. Jevrejeva, J. Moore, and A. Grinsted, J. Geophys. Res. **108**, 4677 (2003).
[55] B. F. Farrell and P. J. Ioannou, J. Atmos. Sci. **50**, 4044 (1993); M. Newman, P. D. Sardeshmukh, and C. Penland, *ibid.* **54**, 435 (1997).
[56] D. N. Mukhin, A. M. Feigin, E. M. Loskutov, and Ya. I. Molkov, Phys. Rev. E **73**, 036211 (2006); E. M. Loskutov, Ya. I. Molkov, D. N. Mukhin, and A. M. Feigin, *ibid.* **77**, 066214 (2008); Y. I. Molkov, E. M. Loskutov, D. N. Mukhin, and A. M. Feigin, *ibid.* **85**, 036216 (2012).
[57] *Climate Change 2013: The Physical Science Basis. Contribution of Working Group I to the Fifth Assessment Report of the Intergovernmental Panel on Climate Change*, edited by T. F. Stocker, D. Qin, G.-K. Plattner *et al.* (Cambridge University Press, Cambridge, 2013).
[58] M. J. McPhaden, S. E. Zebiak, and M. H. Glantz, Science **314**, 1740 (2006).
[59] K.-K. Tung and J. Zhou, Proc. Natl. Acad. Sci. (USA) **110**, 2058 (2013).
[60] I. I. Mokhov, A. V. Eliseev, and D. V. Khvorost'yanov, Izv. Atmos. Ocean. Phys. **36**, 681 (2000).
[61] I. I. Mokhov, D. V. Khvorostyanov, and A. V. Eliseev, Int. J. Climatol. **24**, 401 (2004).
[62] R. A. Kerr, Science **288**, 1984 (2000).
[63] T. L. Delworth and M. E. Mann, Clim. Dyn. **16**, 661 (2000).
[64] M. Dima and G. Lohmann, J. Climate **20**, 2706 (2007).
[65] P. Chylek, C. K. Folland, H. A. Dijkstra, G. Lesins, and M. K. Dubey, Geophys. Res. Lett. **38**, L13704 (2011).
[66] B. Goswami, N. Marwan, G. Feulner, and J. Kurths, Eur. Phys. J. Spec. Top. **222**, 861 (2013).
[67] G. Schwarz, Ann. Stat. **6**, 461 (1978).